Advances in Engineering Software 100 (2016) 308–318

Contents lists available at ScienceDirect

Advances in Engineering Software

journal homepage: www.elsevier.com/locate/advengsoft

Mesh-independent equivalent domain integral method for *J*-integral evaluation

G.P. Nikishkov[a,*], A.V. Vershinin[a,b], Y.G. Nikishkov[c]

[a] *Fidesys LLC, Moscow, Russia*
[b] *Lomonosov Moscow State University, Moscow, Russia*
[c] *University of Texas at Arlington, Arlington, TX, USA*

ARTICLE INFO

Article history:
Received 28 April 2016
Revised 28 July 2016
Accepted 10 August 2016
Available online 13 August 2016

Keywords:
Equivalent domain integral method
J-Integral
Stress intensity factors
Moving least squares
Finite element method
Hexahedral elements
Tetrahedral elements

ABSTRACT

The equivalent domain integral method is a reliable tool for *J*-integral computation in two- and three-dimensional elastic and elastic-plastic fracture mechanics problems. A variant of this method that is independent of finite element mesh is presented. Finite element solution of a boundary value problem is performed on a mesh composed of arbitrary elements. Nodal results are approximated by the moving least squares method that does not require knowledge of mesh topology. Domain integrals are evaluated on a background mesh of hexahedral elements. The mesh has the polar structure with the refinement towards the crack front. Elements of the background mesh are generated in the coordinate system associated with the crack front and then transformed to the global system. Domain integration for each background element is performed once during computations. Evaluation of *J*-integral for multiple domains is achieved by multiplication of an element domain integral with multiple domain weight functions. Performance of the proposed algorithm is demonstrated by the examples of three-dimensional cracks using meshes of both hexahedral and tetrahedral elements.

1. Introduction

The *J*-integral [1,2] is a universal fracture mechanics parameter that can be used both in elastic and elastic-plastic fracture mechanics. Basic definition of the *J*-integral assumes its calculation along a small contour around the crack tip in a two-dimensional case or around a point on the crack front in three-dimensional problems. Using finite element results to calculate the *J*-integral along a small contour can lead to considerable errors [3,4]. The equivalent domain integral (EDI) method [5–8] allows obtaining *J*-integral values with better accuracy. In this method an integral along a small contour is transformed to area or volume domain integral containing special weight function with zero value at the external domain boundary.

Usually domain integral methods are implemented with the use of quadrilateral (2D) or hexahedral (3D) elements. The most popular approach includes: polar mesh refinement around the crack tip (front), use of quadrilateral (hexahedral) elements with quadratic shape functions, and surrounding the crack tip with singular quarter-point elements [9]. The *J*-integral is computed by integration inside finite elements. Thus the boundaries of the integration domain are composed of finite element faces. For example, there is a special three-dimensional crack object in the ANSYS general purpose finite element software [10]. The crack object is a curvilinear cylinder around the crack front filled with the polar mesh of quadratic hexahedral elements. The crack object is inserted into the generated finite element mesh by removing some elements and connecting surface of the crack object with the rest of the mesh.

The EDI method that uses meshes consisting of quadratic hexahedral elements with polar refinement around the crack front, allows obtaining fracture mechanics parameters with high precision. However, difficulties with generation of hexahedral polar meshes motivate researchers to develop variants of EDI methods that work on tetrahedral finite element meshes.

Direct computation of the equivalent domain integral on a mesh of quadratic tetrahedral elements was performed in [11]. Such straightforward approach resulted in large oscillation of *J*-integral values along the crack front. Two modifications were proposed to improve the results. First, the integration domain along the crack front should have the size of four elements. Second, gradients of the domain weight function should be calculated analytically, except for the elements at the boundaries of integration domain where nodal support is used. Such modifications lead to reducing the oscillations of *J*-integral values, however, not to the

* Corresponding author.
E-mail address: nikishkov@gmail.com (G.P. Nikishkov).

http://dx.doi.org/10.1016/j.advengsoft.2016.08.006
0965-9978/

Nomenclature

a	crack size
$\mathbf{c}_k$	unit vectors along axes $\tilde{x}_1\tilde{x}_2$ of the crack front coordinates
d_I	distance between two points
d_{mI}	size of a support domain
E	Young's modulus
f	area under the domain weight function on the crack front
f_i	body forces
J_{III}	energy release rate of the third type
H	effective elasticity modulus
J_1, J_2	components of the J-integral
K_I, K_{II}, K_{III}	stress intensity factors
N^I	element shape functions
n_i	components of a normal to the contour
$\mathbf{p}$	basis for MLS approximation
q	domain weight function
$\mathbf{q}_k$	vector domain weight functions
t_i	crack face tractions
u_i	displacements
W	strain energy density
$w_I(\mathbf{x})$	weight functions for MLS approximation
$w^{(T)}$	weights for Gauss integration
$\tilde{x}_i$	local crack front coordinates
x_i	global coordinates
α_{ij}	direction cosines for coordinate transform
ε_{ij}	strain components
ε^e_{ij}	elastic strains
ε^p_{ij}	plastic strains
ε^t_{ij}	thermal strains
μ	shear modulus
ν	Poisson's ratio
ξ, η, ζ	element local coordinates
ρ	dimensionless distance
σ	remote tension stress applied to the specimen
σ_{ij}	stress components
$\Phi_I(\mathbf{x})$	shape functions for MLS approximation

satisfactory level. The authors of [12] recommended specifying weight function at the nodes of tetrahedral elements and to interpolate it linearly inside the elements. Their main recommendation was related to the size of integration domain along the crack front. This size should be from 6–14 h, where h is the element size along the crack front.

Another approach that avoids meshing with hexahedral elements assumes full independence of the finite element mesh. Chervenka and Saouma [13] proposed to calculate the domain integral in cylindrical domains around the crack front independent of the finite element mesh. The cylinder height was selected equal to the element size along the crack front. Integration was performed in polar coordinates using the special Gauss rule. It was mentioned that displacement derivatives were smoothed but smoothing methodology was not described.

Nagai et al., [14] demonstrated the J-integral computations on tetrahedral meshes using both contour and domain integration independent of the finite element mesh. The moving least squares (MLS) method with weights was employed for approximation of displacements and their derivatives. Neighbor nodes inside a sphere were selected for approximation at the current point. The sphere size was related to the element size where the point was located. Stress intensity factors for mixed-mode problems were obtained by the interaction integral method [15,16].

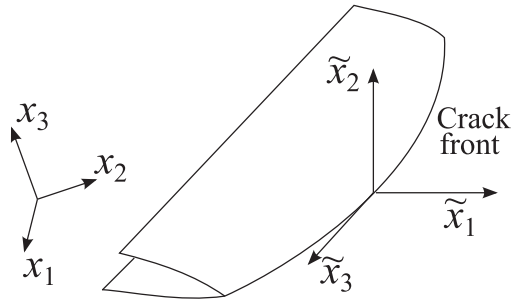

Fig. 1. Global coordinate system $x_1x_2x_3$ and local coordinates $\tilde{x}_1\tilde{x}_2\tilde{x}_3$ for a point at the crack front.

Recent works on the domain integral algorithms in three-dimensional mixed-mode crack problems are mostly based on the interaction integral method where stress intensity factors are calculated directly by combining finite element solution with elastic asymptotic fields for mode I, II and III cracks. While this method provides some convenience, it restricts the use of such domain integral algorithms to elastic problems. The J-integral is applicable to both elastic and elastic-plastic structural integrity assessments [17]. A fracture criterion can be formulated in terms of the J-integral for mode I and mixed-mode problems.

This paper presents further development of the mesh-independent equivalent domain integral method with moving least squares approximation of integrands. In our algorithm of the equivalent domain integral method, the J-integral components J_1 and J_2 are computed in the form suitable for elastic and elastic-plastic cracks. Domain integrals are estimated in the global coordinate system. The J-integral components in the crack front coordinate system are obtained using vector weight function. Calculation of the J_2 requires integration of the strain energy density over the crack surfaces. The special integration rule with double coordinate change removes singularity from the integrand and provides higher accuracy for the J_2 component. If elastic stress intensity factors are necessary, they are determined using components of the J integral and mode III energy release rate. The latter is also estimated by the domain integral method.

In Section 2 the equations of the equivalent domain integral for an arbitrary crack are derived in the global coordinate system. Algorithms of finding the axes of the crack front coordinate system and computing the domain integrals are presented. The moving least squares method and its implementation are discussed in Section 3. Section 4 contains numerical results for an edge cracked plate, penny shaped crack, semi-elliptical surface crack, and inclined penny shaped crack under tensile loading. Comparisons of results obtained on meshes of hexahedral and tetrahedral elements are presented.

2. Algorithm of the equivalent domain integral method

2.1. Equivalent domain integral

Consider a crack in a three-dimensional body with global coordinate system $x_1x_2x_3$ shown in Fig. 1. Local coordinate system $\tilde{x}_1\tilde{x}_2\tilde{x}_3$ is introduced at arbitrary point of the crack front. Coordinate axes $\tilde{x}_1$ and $\tilde{x}_2$ lie in a plane normal to the crack front, $\tilde{x}_2$ is perpendicular to the crack surface, and $\tilde{x}_3$ is tangent to the crack front.

According to the basic definition of J-integral [1], it should be computed along a small contour Γ_ε around the crack front in $\tilde{x}_1\tilde{x}_2$ plane

$$J_k = \int_{\Gamma_\varepsilon} \left(W\tilde{n}_k - \tilde{\sigma}_{ij}\frac{\partial \tilde{u}_i}{\partial \tilde{x}_k}\tilde{n}_j \right) d\Gamma\,, \qquad k = 1,\ 2. \tag{1}$$

Here W is the density of work of stresses on mechanical strains, $\tilde{\sigma}_{ij}$ are stresses, $\tilde{u}_i$ are displacements, and $\tilde{n}_j$ are components of the external normal to the contour Γ_ε. All magnitudes are related to the crack front coordinate system $\tilde{x}_1\tilde{x}_2\tilde{x}_3$.

Two components J_1 and J_2 are sufficient to formulate fracture criteria for general cracks in elastic and elastic-plastic solids. If it is necessary to determine the stress intensity factors K_I, K_{II} and K_{III}, it is possible to define the energy release rate J_{III}

$$J_{III} = \int_{\Gamma_\varepsilon} \left(W_{III}\tilde{n}_1 - \tilde{\sigma}_{3j}\frac{\partial \tilde{u}_3}{\partial \tilde{x}_1}\tilde{n}_j \right) d\Gamma, W_{III} = \frac{1}{2}(\tilde{\sigma}_{3i}\tilde{\varepsilon}^e_{3i}). \tag{2}$$

Then the stress intensity factors are calculated as follows:

$$K_{I/II} = \frac{1}{2}\sqrt{H}\left(\sqrt{J_1 - J_2 - J_{III}} \pm \sqrt{J_1 + J_2 - J_{III}}\right), \quad K_{III} = \sqrt{2\mu J_{III}} \tag{3}$$

where $\mu = E/(2(1+\nu))$ is the shear modulus, H is the effective elasticity modulus, which is equal to Young's modulus E for plane stress and $E/(1-\nu^2)$ for plane strain conditions.

For an arbitrary three-dimensional crack it is natural to perform computations in the global coordinate system $x_1x_2x_3$. The J-integral can be expressed in the global coordinate system [16]

$$J_k = c_{kl}\int_{\Gamma_\varepsilon}\left(W\delta_{lj} - \sigma_{ij}\frac{\partial u_i}{\partial x_l}\right)n_j\, d\Gamma\,, \qquad k = 1,\ 2 \tag{4}$$

where c_{kl} are components of the unit vectors $\mathbf{c}_k$ that are oriented along axes $\tilde{x}_1$ and $\tilde{x}_2$ of the coordinate system associated with the crack front.

Computation of the integral along a small contour using the finite element solution can lead to considerable errors. The equivalent domain integral method [5–8] replaces a small contour integral by a domain integral over the large area or volume. In addition, the domain (area or volume) integration is better suited for implementation using the finite element method.

Let us assume that the crack surface is loaded by tractions t_i, and the solid is subjected to body forces f_i and a temperature field. In case of elastic-plastic deformation, total strains can be decomposed into the following sum

$$\varepsilon_{ij} = \varepsilon^e_{ij} + \varepsilon^p_{ij} + \varepsilon^t_{ij} \tag{5}$$

where superscripts e, p and t denote elastic, plastic, and thermal fractions. Density of stress work on mechanical strains W is

$$W = \int \sigma_{ij} d\varepsilon^{ep}_{ij}. \tag{6}$$

Here ε^{ep}_{ij} is a sum of elastic ε^e_{ij} and plastic ε^p_{ij} strains. If constitutive material equations are described by the deformation or flow theory under the proportional loading then stresses can be expressed through the energy density W

$$\sigma_{ij} = \frac{\partial W}{\partial \varepsilon^{ep}_{ij}}. \tag{7}$$

Using the divergence theorem and taking into account equilibrium equations, it is possible to transform the contour integral (4) into its equivalent domain representation

$$\begin{aligned} J_k &= J_k(q) + J_k(V) + J_k(A_c), \\ J_k(q) &= -\frac{1}{f}\int_{V-V_\varepsilon}\left(W\delta_{lj} - \sigma_{ij}\frac{\partial u_i}{\partial x_l}\right)\frac{\partial q_{kl}}{\partial x_j}dV, \\ J_k(V) &= \frac{1}{f}\int_{V-V_\varepsilon}\left(\sigma_{ij}\frac{\partial \varepsilon^t_{ij}}{\partial x_l} - f_i\frac{\partial u_i}{\partial x_l}\right)q_{kl}\, dV, \\ J_k(A_c) &= \frac{1}{f}\int_{A_c}\left(\delta_{k2}Wn_l - t_i\frac{\partial u_i}{\partial x_l}\right)q_{kl}\, dA. \end{aligned} \tag{8}$$

Here δ_{lj} is the Kronecker delta. Integration domain $V - V_\varepsilon$ around the front segment and crack surfaces A_c are shown in Fig. 2. The

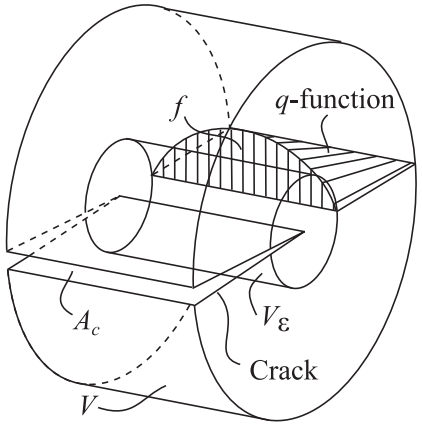

Fig. 2. Equivalent domain integration around a segment of the crack front. Radial section of the weight function q is shown.

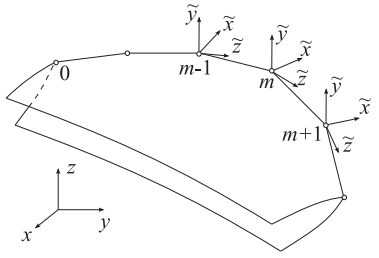

Fig. 3. Global coordinate system xyz and local coordinate system $\tilde{x}\tilde{y}\tilde{z}$ at nodes at the crack front.

weight function q is selected such that it is equal to zero on external and side surfaces of the integration domain. Area f under q-function on the inner surface of the integration domain is calculated as

$$f = \int q\, ds \tag{9}$$

where s is a coordinate along the crack front. Components q_{kl} of the vector functions $\mathbf{q}_k$ are equal to

$$q_{kl} = c_{kl}q. \tag{10}$$

Second term of (8) is necessary when thermal strains ε^t_{ij} or volume forces f_i are present. Additional area integration over the crack surface A_c is required for the second component of the J-integral and when surface tractions t_i act on the crack faces.

2.2. Crack front coordinate system at nodes

The crack front is defined by the vertices numbered according to the distance from an arbitrary starting point 0 as shown in Fig. 3. Origin of the local coordinate system $\tilde{x}\tilde{y}\tilde{z}$ $(=\tilde{x}_1\tilde{x}_2\tilde{x}_3)$ can be attached to any vertex of the crack front. Axes $\tilde{x}$ and $\tilde{y}$ lie in the plane that is normal to the crack front. Axis $\tilde{y}$ is perpendicular to the crack surface. Axis $\tilde{z}$ is tangent to the crack front.

Let us consider how to determine the orientation of the crack front coordinate system when the crack front is defined by straight segments and the crack surface is defined by flat element faces. We start with the determination of $\mathbf{z}$ that is unit vector along the local coordinate $\tilde{z}$ at vertex $\mathbf{v}_m$.

Fig. 4 shows the top view of the crack front. First, vectors $\mathbf{z}_{m-1,m}$ and $\mathbf{z}_{m,m+1}$ along two neighboring segments of the crack front are determined

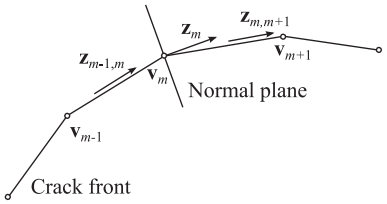

Fig. 4. Finding orientation of z-axis.

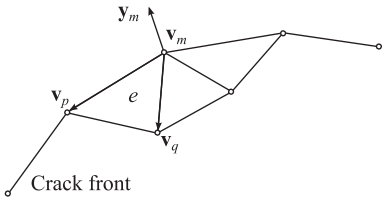

Fig. 5. Finding orientation of y-axis.

$$\mathbf{z}_{m-1,m} = \frac{\mathbf{v}_m - \mathbf{v}_{m-1}}{\|\mathbf{v}_m - \mathbf{v}_{m-1}\|},$$
$$\mathbf{z}_{m,m+1} = \frac{\mathbf{v}_{m+1} - \mathbf{v}_m}{\|\mathbf{v}_{m+1} - \mathbf{v}_m\|} \tag{11}$$

where $\mathbf{v}_{m+1}$, $\mathbf{v}_m$ and $\mathbf{v}_{m-1}$ are crack front vertex coordinates, and $\|\cdot\|$ denotes vector length. Orientation of the axis z at the crack front node m is obtained by averaging the two vectors above

$$\mathbf{z}_m = \{a_m\ b_m\ c_m\} = \frac{1}{2}(\mathbf{z}_{m-1,m} + \mathbf{z}_{m,m+1}). \tag{12}$$

Equation for a plane normal to the crack front at vertex m can be written in the standard form using the components of its normal a_m, b_m and c_m

$$a_m x + b_m y + c_m z + d_m = 0,$$
$$d_m = -(a_m x_m + b_m y_m + c_m z_m). \tag{13}$$

Estimation of y_m and x_m orientations at the crack front nodes is based on the orientation of element faces at the crack surface. We find element faces at the crack surface that include vertex m. For each face e a normal $\mathbf{y_e}$ is determined as a normalized vector product of the two edges as demonstrated in Fig. 5. Approximation $\mathbf{y}_m^{(1)}$ is found by averaging the normals $\mathbf{y_e}$

$$\mathbf{y}_e = \frac{(\mathbf{v}_p - \mathbf{v}_m) \times (\mathbf{v}_q - \mathbf{v}_m)}{\|(\mathbf{v}_p - \mathbf{v}_m) \times (\mathbf{v}_q - \mathbf{v}_m)\|},$$
$$\mathbf{y}_m^{(1)} = \frac{1}{n}\sum \mathbf{y}_e. \tag{14}$$

Since $\mathbf{y}_m^{(1)}$ is not necessarily located in the normal plane at the crack front node, we project it on the normal plane and normalize

$$\mathbf{y_m^{(2)}} = \mathbf{y}_m^{(1)} - \left(\mathbf{y}_m^{(1)} \cdot \mathbf{z}_m\right)\mathbf{z}_m,$$
$$\mathbf{y}_m = \frac{\mathbf{y}_m^{(2)}}{\left\|\mathbf{y}_m^{(2)}\right\|}. \tag{15}$$

Finally $\mathbf{x}_m$ is found as a vector product of axes $\mathbf{y}_m$ and $\mathbf{z}_m$

$$\mathbf{x}_m = \mathbf{y}_m \times \mathbf{z}_m. \tag{16}$$

2.3. Domain integration

Our integration algorithm is independent of a finite element mesh used for solution of elastic or elastic-plastic problem. For domain integration, we introduce a background polar mesh of linear hexahedral 8-node elements around the crack front as shown in Fig. 6. Integration domains are composed of cylinders located between two planes that are normal to the crack front and pass through nodes. Integration elements are generated in the local coordinate system where coordinate $\tilde{z}$ is always zero. Then nodal coordinates are transformed to the global coordinate system using direction cosines $\alpha_{ij} = \cos(\tilde{x}_i, x_j)$

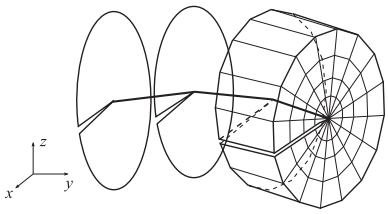

Fig. 6. Background mesh of hexahedral linear elements in the global coordinate system.

$$x_i = \alpha_{ji}\tilde{x}_j + x_j^C \tag{17}$$

where x_j^C are global coordinates of the node at the crack front. Different direction cosines are used for element nodes that belong to different planes in the global coordinate system.

A global to local transformation matrix at node m is defined by unit vectors $\mathbf{x}_m$, $\mathbf{y}_m$ and $\mathbf{z}_m$ of the local coordinate axes $\tilde{x}\tilde{y}\tilde{z}$

$$\alpha_{\mathbf{m}} = \begin{bmatrix} \mathbf{x}_m \\ \mathbf{y}_m \\ \mathbf{z}_m \end{bmatrix}. \tag{18}$$

In Eq. (17) the transposed matrix of direction cosines α_{ji} is used because of the transformation from local to global coordinates.

Calculation of domain integrals (8) is performed for all elements using the shape functions for interpolation of the domain weight function q. For the linear hexahedral element, the shape functions N^I are

$$N^I = \frac{1}{8}(1 + \xi\xi_I)(1 + \eta\eta_I)(1 + \zeta\zeta_I) \tag{19}$$

where ξ, η, ζ are local element coordinates in the range $[-1, 1]$ and ξ_I, η_I, ζ_I are their values at nodes.

Interpolation of the weight function q is done as follows

$$q = N^M q^M. \tag{20}$$

From the above relation it is possible to find derivatives of the weight function

$$\frac{\partial q}{\partial x_j} = \frac{\partial N^M}{\partial x_j} q^M, \tag{21}$$

and components of the vector functions $\mathbf{q_k}$

$$\frac{\partial q_{kl}}{\partial x_j} = \frac{\partial N^M}{\partial x_j} q_{kl}^M. \tag{22}$$

Integration of components $J_k(q)$ in (8) for one finite element in the local element coordinates ξ, η, ζ becomes

$$J_k(q) = -\frac{1}{f}\int_{-1}^{1}\int_{-1}^{1}\int_{-1}^{1}\left(W\delta_{lj} - \sigma_{ij}\frac{\partial u_i}{\partial x_l}\right)\frac{\partial N^M}{\partial x_j} q_{kl}^M \det J d\xi d\eta d\zeta \tag{23}$$

where $\det J$ is a determinant of the Jacobi matrix. Nodal vector q_{kl}^M can be moved outside of the integral, which allows performing efficient computation of $J_k(q)$ for multiple weight functions q using the Gauss integration rule

$$J_k(q) = R_l^M q_{kl}^M,$$
$$R_l^M = -\frac{1}{f}\left[\left(W\delta_{lj} - \sigma_{ij}\frac{\partial u_i}{\partial x_l}\right)\frac{\partial N^M}{\partial x_j}\det J\right]^{(T)} w^{(T)}. \tag{24}$$

Here (T) denotes expressions at integration points, and $w^{(T)}$ are integration weights. In the linear elastic case, only the nodal displacements are necessary for the integral (24). Displacement derivatives $\partial u_i/\partial x_l$ are approximated using the moving least squares method; stresses σ_{ij} and elastic energy density W are determined by Hook's law. Elastic-plastic case requires moving least squares approximation of stresses and work density from the finite element solution. Since all quantities can be determined at any point, it is possible to use any number of integration points in an element.

Estimation of $J_k(V)$ is performed in a similar way

$$J_k(V) = S_l^M q_{kl}^M,$$
$$S_l^M = \frac{1}{f}\left[\left(\sigma_{ij}\frac{\partial \varepsilon_{ij}^t}{\partial x_l} - f_i\frac{\partial u_i}{\partial x_l}\right)N^M \det J\right]^{(T)} w^{(T)}. \tag{25}$$

Components $J_k(A_c)$ are integrated over element faces that are located on the crack surfaces A_c:

$$J_k(A_c) = T_l^M q_{kl}^M,$$
$$T_l^M = \frac{1}{f}\left[\left(\delta_{k2} W n_l - t_i\frac{\partial u_i}{\partial x_l}\right)N^M \det J\right]^{(t)} w^{(t)}. \tag{26}$$

Superscript (t) is used to denote the integration points on element faces.

Computing the J-integral in the form (24,25,26) allows using multiple weight functions for the current element of the integration domain. The following weight function q was selected in this study

$$q(r,\tilde{x}_3) = \begin{cases} \left(1 - \dfrac{|\tilde{x}_3|}{h}\right), & r_0 < r \le r_1, \\ \left(1 - \dfrac{|\tilde{x}_3|}{h}\right)\left(\dfrac{r_2 - r}{r_2 - r_1}\right), & r_1 < r \le r_2. \end{cases} \tag{27}$$

Here r and $\tilde{x}_3$ are radial distance and local coordinate along the crack front, respectively, and, h is half size of the integration domain along the crack front ($-h \le \tilde{x}_3 \le h$). The q-function is linear in the $\tilde{x}_3$ direction on each side from the central point. It is constant in the radial direction from r_0 to r_1 and linear from r_1 to r_2. According to the definition of the J-integral (1), r_0 should be small compared to the crack size.

2.4. Integration of the strain energy density over the crack surface

Calculation of the integral (26) over the crack surface presents considerable difficulties because the integration domain starts at the crack front, and the integrand contains a singular function $W(r)$. Consider the integration of the strain energy density W, which is necessary for determining the value of J_2

$$I = \int_{A_c} W dA. \tag{28}$$

The function of the elastic energy density W has singularity $1/r$, where r is the distance from the crack front. Therefore, the integrals along each of the crack surfaces are divergent. However, the energy difference between the upper and lower crack surfaces $\Delta W = W_+ - W_-$ is characterized by the singularity of $1/\sqrt{r}$ [18], and the integral along the crack area has a finite value. Thus, we need to obtain the value of the integral

$$I = \int_C \Delta W dA. \tag{29}$$

where C is one (upper or lower) of the crack surfaces.

Eischen [18] proposed a method for computing such integral in the two-dimensional case. His method uses analytical expression for the strain energy difference near the crack tip and requires two integrations over the crack line for determining two unknown constants.

Here we propose to determine the integral (29) using a special integration rule, which removes singularity in the integrand. Similar approach was employed by Walters et al., [19] for integration of the crack surface traction term in Eq. (26).

A direct calculation of the integral over finite elements using Gauss integration rule gives acceptable results with the exception of the elements directly adjacent to the crack front. For a two-dimensional element next to the crack front, singularity can be removed by the coordinate change. The integral over the two-dimensional element has the form

$$I = \int_{-1}^{1}\int_{-1}^{1} F(\xi,\eta) d\xi d\eta. \tag{30}$$

where $F(\xi,\eta) = \Delta W(\xi,\eta)\det J(\xi,\eta)$. Suppose that the local coordinate ξ is oriented along the radial direction. After a change of the coordinate $\xi = \omega^2 - 1$, the integral becomes nonsingular

$$I = \int_0^{\sqrt{2}}\int_{-1}^{1} 2\omega F(\omega^2 - 1,\eta) d\omega d\eta. \tag{31}$$

To have the standard limits of integration, we make another change of variable $\omega = (1+\zeta)/\sqrt{2}$. Then the integral becomes

$$I = \int_{-1}^{1}\int_{-1}^{1} (1+\zeta) F\left(\frac{1}{2}\left(\zeta^2 + 2\zeta - 1\right), \eta\right) d\zeta d\eta. \tag{32}$$

Efficiency of the integration rule with double coordinate change can be demonstrated by estimating the integral $I = \int_0^1 r^{-1/2} dr$. Usual Gauss rule with 2, 3 and 4 integration points gives integral values 1.651, 1.751, and 1.806, respectively. Special integration rule provides correct result $I = 2$ even for one integration point.

Special integration (32) requires the values of ΔW at small distances from the crack front. Direct calculation of the energy density near the crack front by the moving least squares can lead to significant errors.

To estimate the energy density difference near the crack front, it is possible to use the value of ΔW at some point r_2 farther away. This point should not be too far from the crack front since the strain energy density difference should still follow its asymptotic behavior. Suppose that we need the value of ΔW_1 at a point, located at distance r_1 from the crack front. Since the radial dependence of ΔW is given by

$$\Delta W = \frac{k}{\sqrt{r}} \tag{33}$$

then the following relation

$$\Delta W_1 = \frac{\Delta W_2 \sqrt{r_2}}{\sqrt{r_1}} \tag{34}$$

can be used for estimation of the strain energy density in the vicinity of the crack front. Numerical experiments show that the optimal distance r_2 is 1.25 times the size of the integration element adjacent to the crack front. The above procedure can be also applied to estimation of the second term in Eq. (26) since it requires surface integration of displacement derivatives with the square root singularity.

3. MLS approximation

3.1. Moving least squares method

Approximation of displacement derivatives and other quantities necessary for J-integral estimation is done according to the moving least squares (MLS) method, which is widely used in the meshless finite element method [20].

Let a scalar function u be specified as u_I at nodes $\mathbf{x_I}$. Function approximation $u^h(\mathbf{x})$ with error minimization in the least square sense can be represented in the form

$$u^h(\mathbf{x}) = \sum_j^m p_j(\mathbf{x}) a_j(\mathbf{x}) = \mathbf{p}^T(\mathbf{x})\mathbf{a}(\mathbf{x}) \tag{35}$$

where $\mathbf{p}$ is a basis, which contains approximating functions. If a weight function is introduced for nodal points $w(\mathbf{x}-\mathbf{x}_I) = w_I(\mathbf{x})$ then the unknown vector $\mathbf{a}$ $(\mathbf{x})$ becomes equal to

$$\mathbf{a}(\mathbf{x}) = \mathbf{A}^{-1}(\mathbf{x})\mathbf{B}(\mathbf{x})\mathbf{U} \tag{36}$$

after minimizing the sum of squares of deviations. Here the following notations were used

$$\begin{aligned}
\mathbf{A}(\mathbf{x}) &= \sum_I^n w_I(\mathbf{x})\mathbf{p}(\mathbf{x}_I)\mathbf{p}^T(\mathbf{x}_I),\\
\mathbf{B}(\mathbf{x}) &= [w_1(\mathbf{x})\mathbf{p}(\mathbf{x}_1)\ \ w_2(\mathbf{x})\mathbf{p}(\mathbf{x}_2)\ \ \ldots\ \ w_n(\mathbf{x})\mathbf{p}(\mathbf{x}_n)],\\
\mathbf{U} &= \{u_1\ \ u_2\ \ \ldots\ \ u_n\}.
\end{aligned} \tag{37}$$

Function approximation

$$\mathbf{u}^h(\mathbf{x}) = \sum_I^n \sum_j^m p_j(\mathbf{x})\left(\mathbf{A}^{-1}(\mathbf{x})\mathbf{B}(\mathbf{x})\right)_{jI}\mathbf{u}_I \tag{38}$$

can be represented in the form of shape function interpolation

$$\mathbf{u}^h(\mathbf{x}) = \sum_I^n \phi_I(\mathbf{x})\ \mathbf{u}_I. \tag{39}$$

Shape functions are given by the following expression

$$\phi_I(\mathbf{x}) = \sum_j^m p_j(\mathbf{x})\left(\mathbf{A}^{-1}(\mathbf{x})\mathbf{B}(\mathbf{x})\right)_{jI}. \tag{40}$$

In vector notation, this can be rewritten as

$$\begin{aligned}
\Phi(\mathbf{x}) &= \mathbf{g}^T(\mathbf{x})\mathbf{B}(\mathbf{x}),\\
\mathbf{g}(\mathbf{x}) &= \mathbf{A^{-1}}(\mathbf{x})\mathbf{p}(\mathbf{x}).
\end{aligned} \tag{41}$$

Shape function derivatives are obtained by differentiation of the above expression

$$\begin{aligned}
\frac{\partial\Phi(\mathbf{x})}{\partial x_i} &= \left(\frac{\partial\mathbf{g}}{\partial x_i}\right)^T\mathbf{B} + \mathbf{g}^T\frac{\partial\mathbf{B}}{\partial x_i},\\
\frac{\partial\mathbf{g}}{\partial x_i} &= \mathbf{A^{-1}}\left(\frac{\partial\mathbf{p}}{\partial x_i} - \frac{\partial\mathbf{A}}{\partial x_i}\mathbf{g}\right).
\end{aligned} \tag{42}$$

Derivatives in the above equations are defined by direct differentiation.

3.2. Implementation of the MLS method

In the implementation of the MLS method it is necessary to select the basis $\mathbf{p}$, weight function $w_I(\mathbf{x})$, and to develop algorithm of finding support nodes.

3.2.1. Basis

Linear polynomial basis was selected

$$\mathbf{p}(\mathbf{x}) = \{1\ x\ y\ z\}. \tag{43}$$

Our experiments showed that increasing the polynomial order has little effect on the results of approximation of the displacement field.

3.2.2. Weight function

Various weight functions are used in MLS approximations; among them: Gauss function, spline functions, radial based functions etc. Usually weight functions use dimensionless radius ρ as an argument

$$\begin{aligned}
\rho &= d_I/d_{mI},\\
d_I &= \|\mathbf{x}-\mathbf{x}_I\|
\end{aligned} \tag{44}$$

where d_I is the distance between points $\mathbf{x}$ and $\mathbf{x}_I$, and d_{mI} is a radius of a support domain. In our implementation, we selected Gauss weight function that reads

$$w_I(\mathbf{x}) = w(\mathbf{x}-\mathbf{x}_I) = \frac{\exp\left(-(\beta\rho)^2\right) - \exp\left(-\beta^2\right)}{1-\exp\left(-\beta^2\right)}. \tag{45}$$

Here β is a parameter defining the sharpness of the weight function (typical value is $\beta = 3$).

In the three-dimensional case we use a weight function defined as a product of one-dimensional weight functions [21]

$$w(\mathbf{x}-\mathbf{x}_I) = w(\rho_x)w(\rho_y)w(\rho_z) \tag{46}$$

where ρ_x, ρ_y and ρ_z are

$$\begin{aligned}
\rho_x &= |x-x_I|/d_{mI},\\
\rho_y &= |y-y_I|/d_{mI},\\
\rho_z &= |z-z_I|/d_{mI}.
\end{aligned} \tag{47}$$

3.2.3. Searching support nodes

Results of problem solution are known at the nodes of the finite element mesh. For MLS approximation it is necessary to find the specified number of the nodes closest to the point of approximation. Such nodes are called support nodes, and a region of their location is a support domain.

In our implementation of the MLS method, we use simple basket algorithm for the efficient search of the support nodes. Before performing the computation of the J-integral by the equivalent domain integral method, we create a list of lists which contains node numbers located inside the integration elements. Integration elements are considered as baskets with nodes inside. When support nodes are sought, a basket of the current integration element is used for the support nodes search. If the required support domain becomes larger than the current basket then the neighboring baskets are used.

4. Numerical results

This section contains three-dimensional examples of calculation of stress intensity factors using the developed algorithm of the mesh-independent equivalent domain integral method.

The following problems are considered:

1. Tensile plate with an edge crack
2. Cylinder with a circular crack under tension
3. Semi-elliptical surface crack
4. Inclined circular crack under tension

Each problem is solved twice using hexahedral 20-node elements and tetrahedral 10-node elements.

Hexahedral meshes were created using our specialized mesh generator. They are characterized by a regular mesh structure, polar refinement towards the crack front, and singular quarter-point elements around the crack front.

Tetrahedral meshes were generated using the preprocessor of the general purpose finite element software FIDESYS [22,23]. The theoretical background of CAE FIDESYS, including mechanical and mathematical problem statements, is described in [4,24,25]. Generated tetrahedral meshes are almost completely irregular with the exception of specified size of elements at the crack front.

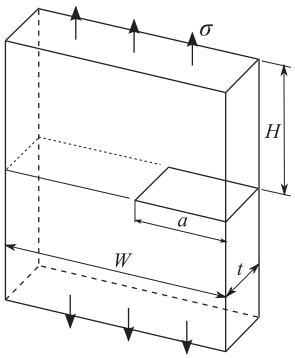

Fig. 7. Plate with an edge crack under tension, $a/W = 0.5$.

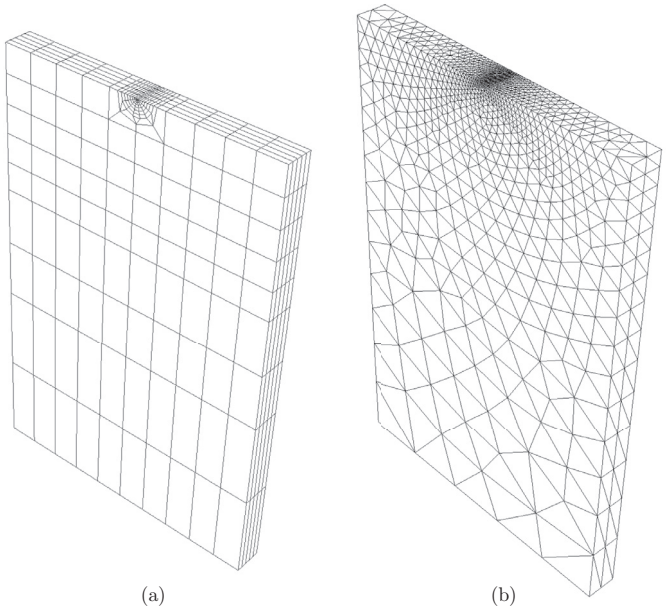

Fig. 8. Meshes for calculation of stress intensity factor for an edge cracked plate: a) 740 quadratic hexahedral elements b) 15,418 quadratic tetrahedral elements.

Calculation of domain integrals (24–26) with bilinear weigh function q (27) does not use topology of the meshes. Only the displacements at nodes are involved in the approximation of displacements, their derivatives, and other quantities at integration points of a background mesh. Integration domains have the size of two elements along the crack front and a multiple of specified size in the radial direction. Radius r_1 in (27) is selected equal to double of the radial size of crack front elements.

4.1. Plate with an edge crack

A plate of width W and thickness t containing a crack of length a under remote tensile stress σ is shown in Fig. 7.

The three-dimensional problem for $a/W = 0.5$, $t/W = 0.1$, $H/W = 1.5$ is solved with zero displacement boundary conditions in the thickness direction on both plate surfaces such that the stress intensity factor K_I is constant along the crack front. Such problem statement allows estimating the influence of tetrahedral mesh irregularity on the scatter of K_I.

A finite element mesh consisting of 740 hexahedral elements and 3789 nodes is presented in Fig. 8a. Polar refinement around the crack front has seven elements in the angular direction. Radial size of singular quarter-point elements is $e_{min} = 0.05t$.

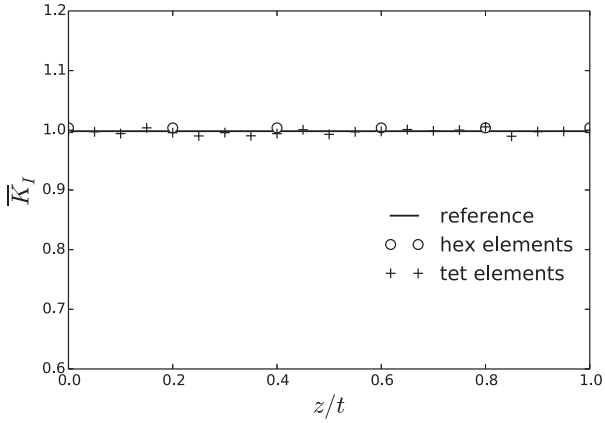

Fig. 9. Stress intensity factor along the front of an edge crack $a/W = 0.5$ in a tensile plate.

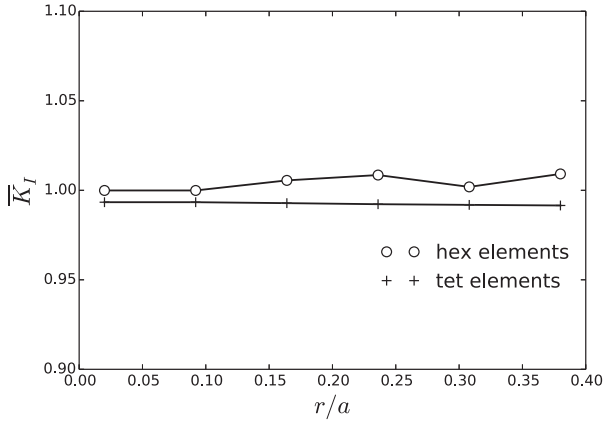

Fig. 10. Dependence of the stress intensity factor on the integration domain radius for an edged crack plate.

Fig. 8b shows the mesh of 15,418 tetrahedral elements and 23,693 nodes. The size of the elements at the crack front is $e_{min} = 0.05t$.

Results for the normalized stress intensity factor $\bar{K}_I$

$$\bar{K}_I = \frac{K_I(1 - a/W)^{3/2}}{\sigma\sqrt{\pi a}}$$

obtained with hexahedral and tetrahedral meshes are compared with the reference solution $\bar{K}_I = 0.9985$ [26] in Fig. 9. Relative difference of K_I determined on the hexahedral mesh from the reference solution is 0.4%. Scatter of results obtained on the tetrahedral mesh is within ± 1%. Fig. 10 shows dependence of the stress intensity factor $\bar{K}_I$ on the radial size of an integration domain r/a. The results are almost independent of integration domain. Higher oscillations of $\bar{K}_I$ values for the hexahedral mesh are explained by large element sizes for $r/a > 0.07$.

4.2. Cylinder with a circular crack

Problem schematic for a cylinder of radius R with a circular crack of radius a under tensile loading σ is presented in Fig. 11. The problem is suitable for testing the algorithm of the equivalent domain integration method since the solution is a constant value of K_I along the curved crack front. Reference value of the normalized stress intensity factor $\bar{K}_I$ for $a/R = 0.2$ is given in [27]

$$\bar{K}_I = \frac{K_I}{2\sigma\sqrt{a/\pi}} = 1.005.$$

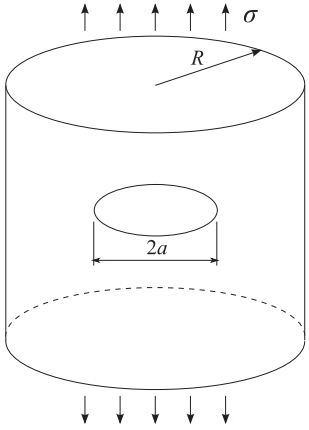

Fig. 11. Circular crack in a tensile cylinder, $a/R = 0.2$.

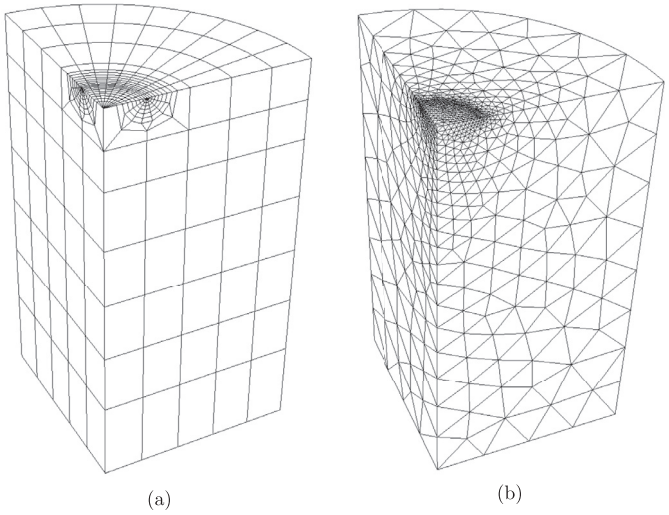

Fig. 12. Meshes for calculation of stress intensity factor for a circular crack in a tensile cylinder: a) 837 quadratic hexahedral elements b) 7111 quadratic tetrahedral elements.

Fig. 12 shows hexahedral (837 elements, 3874 nodes) and tetrahedral (7111 element, 11,062 nodes) meshes. Both meshes have minimal element size $e_{min} = 0.05a$. Results for the stress intensity factor are presented in Fig. 13. The hexahedral mesh gives K_I with an error less than 0.3%. The tetrahedral mesh produces results with maximum error within 2%. Results at the selected crack front vertex for the integration domains with different radial sizes are characterized by high stability.

4.3. Semi-elliptical surface crack

Computation of the stress intensity factor at the front of a semi-elliptical surface crack (Fig. 14) is a typical task in the structural integrity analysis. We consider a semi-elliptical crack with semi-axes a and c in a block of width $2b$ and thickness t under tensile stress σ. The following geometric details are selected: $a/c = 0.5$, $a/t = 0.25$, $a/b = 0.125$.

Finite element meshes consisting of 738 hexahedral elements with 3597 nodes and 10,633 tetrahedral elements with 16,290 nodes are presented in Fig. 15. Radial element size of the quarter-point elements at the crack front in the hexahedral mesh and minimal element size in the tetrahedral mesh are $e_{min} = 0.05a$.

Fig. 16 shows the stress intensity factor K_I on the crack front as a function of elliptical angle ϕ. Values of K_I are normalized as

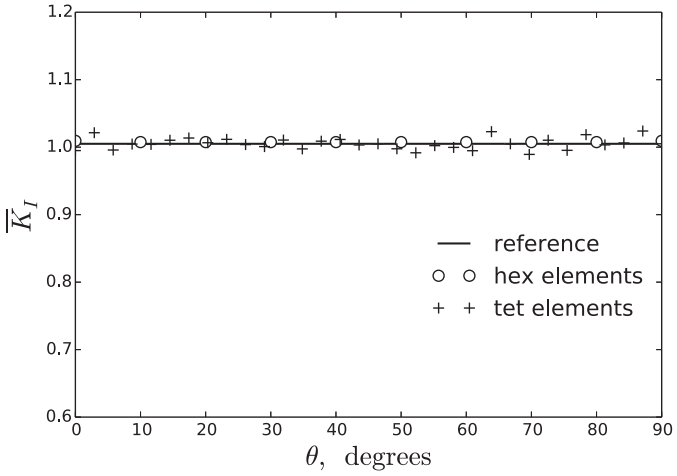

Fig. 13. Stress intensity factor along the front of the circular crack.

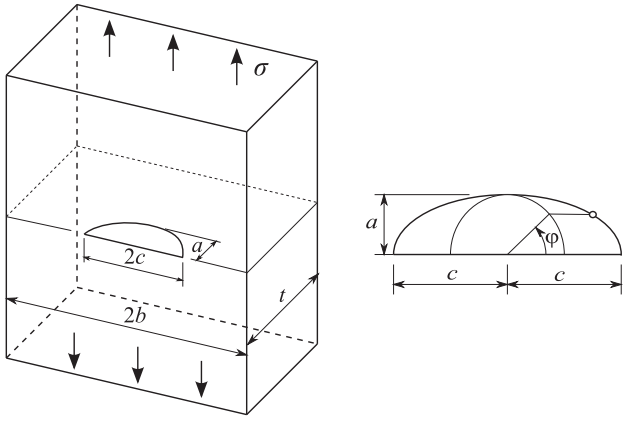

Fig. 14. Semi-elliptical surface crack $a/c = 0.5$ in a tensile block, $a/t = 0.25$, $a/b = 0.125$.

follows:

$$\bar{K}_I = \frac{K_I Q}{\sigma\sqrt{\pi a}},$$

$$Q = \left(1 + 1.464\left(\frac{a}{c}\right)^{1.65}\right)^{1/2}.$$

Results obtained on the hexahedral and tetrahedral meshes demonstrate satisfactory agreement with reference solution [28].

4.4. Inclined circular crack

Schematic of the problem for an inclined circular crack under tension is shown in Fig. 17. This problem is used for demonstration of the proposed algorithm to calculate stress intensity factors K_I, K_{II} and K_{III}, which are given by the following formulas [29] for the case of infinite medium

$$K_I = 2\sigma\sqrt{\frac{a}{\pi}}\cos^2\alpha,$$

$$K_{II} = \frac{2}{2-\nu}\sigma\sqrt{\frac{a}{\pi}}\sin 2\alpha\cos\theta,$$

$$K_{III} = \frac{2(1-\nu)}{2-\nu}\sigma\sqrt{\frac{a}{\pi}}\sin 2\alpha\sin\theta$$

where a is a crack radius, σ is a remote tensile stress, ν is Poisson's ratio, α is an angle between the plane normal to the cylinder axis and the crack plane, and θ is an angle along the crack front.

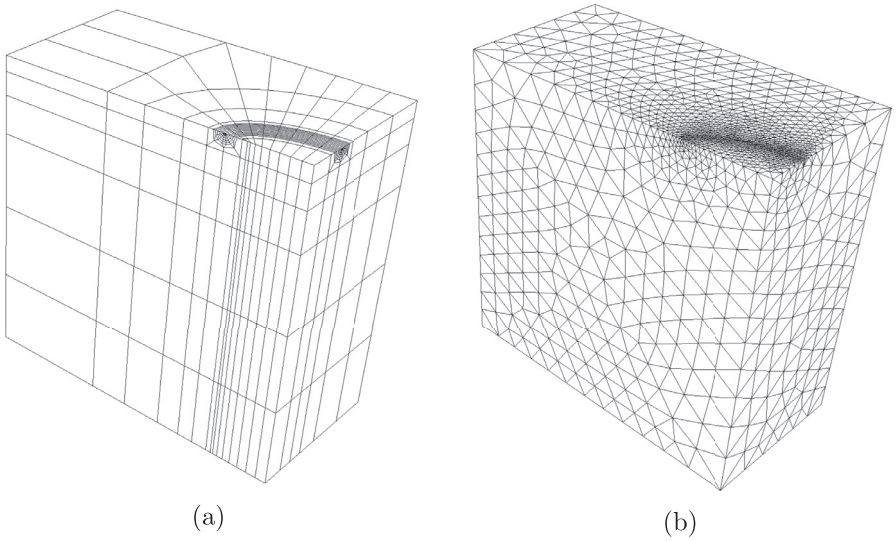

Fig. 15. Meshes for calculation of stress intensity factor for a semi-elliptical surface crack: a) 738 hexahedral elements b) 10,633 tetrahedral elements.

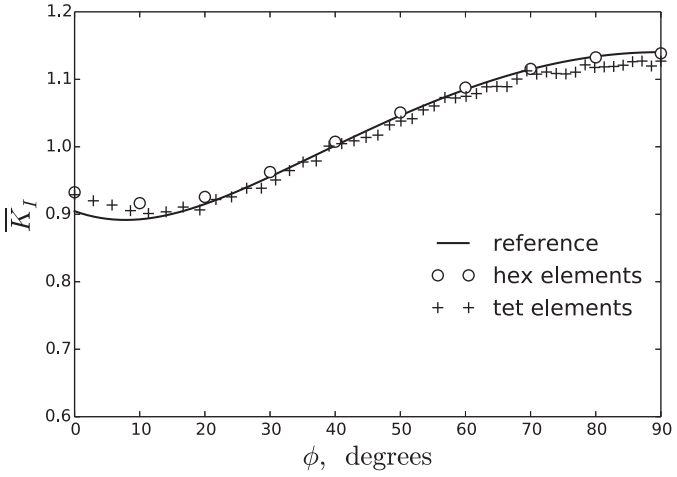

Fig. 16. Stress intensity factor K_I as a function of elliptical angle ϕ for the semi-elliptical surface crack.

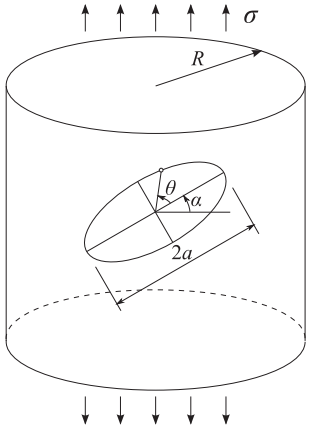

Fig. 17. Inclined circular crack in a tensile cylinder.

Finite element meshes composed of hexahedral and tetrahedral elements are presented in Fig. 18 for $a/R = 0.1$ and $\alpha = 30^\circ$. The hexahedral mesh is composed of 2988 elements and 12,659 nodes. The tetrahedral mesh includes 32,316 elements and 48,015 nodes. Since we generated finite element models with $a/R = 0.1$, it is possible to employ formulas for an infinite medium for the reference purpose.

The components of the J-integral J_1, J_2, and the energy release rate J_{III} are normalized as

$$\bar{J}_i = \frac{J_i}{4\sigma^2 a/(\pi E)}.$$

Comparison of computed values and theoretical solution for an inclined circular crack in an infinite medium [29] is shown in Fig. 19.

Results for stress intensity factors K_I, K_{II} and K_{III} normalized as

$$\bar{K}_i = \frac{K_i}{2\sigma\sqrt{a/\pi}}$$

are given in Fig. 20. Errors for all stress intensity factors are in the acceptable range.

5. Conclusion

A mesh-independent variant of the equivalent domain integral method for estimating components of the J-integral and stress intensity factors K_I, K_{II} and K_{III} is presented. Calculations of domain integrals are performed in the global coordinate system based on the displacements and other data at nodes of the finite element mesh or any other points in space. Regular background mesh of hexahedral elements is introduced around the crack front for domain integration. Vector weight function q is used to obtain components of the J-integral in the local crack front coordinate system. Integration of the strain energy density over the crack surface in the J_2 component is performed with a special algorithm that removes singularity using the double coordinate change. The energy release rate of the third type J_{III} can be computed if it is necessary to separate the stress intensity factors.

Performance of the mesh-independent domain integral method is demonstrated on several numerical examples for three-dimensional cracks. Two types of meshes were generated for each of the crack problems. The first mesh is composed of hexahedral 20-node elements and regular polar mesh around the crack front. Singular quarter-point elements were placed at the crack front. Tetrahedral 10-node elements were used in the second mesh that was irregular except for the specified element size at the crack front. Calculated J-integral values and values of the stress intensity factors are in agreement with reference solutions.

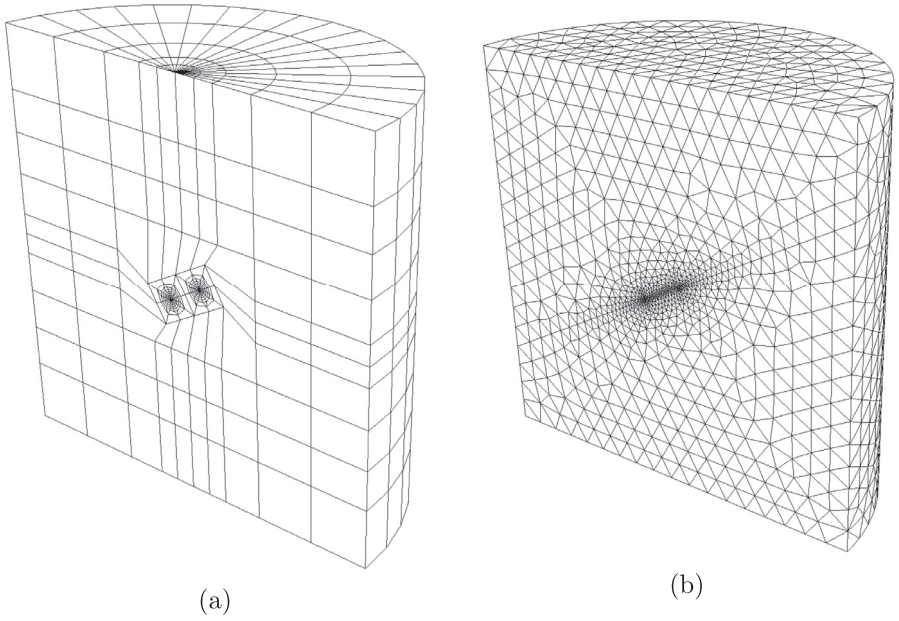

Fig. 18. Meshes for calculation of stress intensity factors for an inclined circular crack: a) 2988 hexahedral elements b) 32,316 tetrahedral elements.

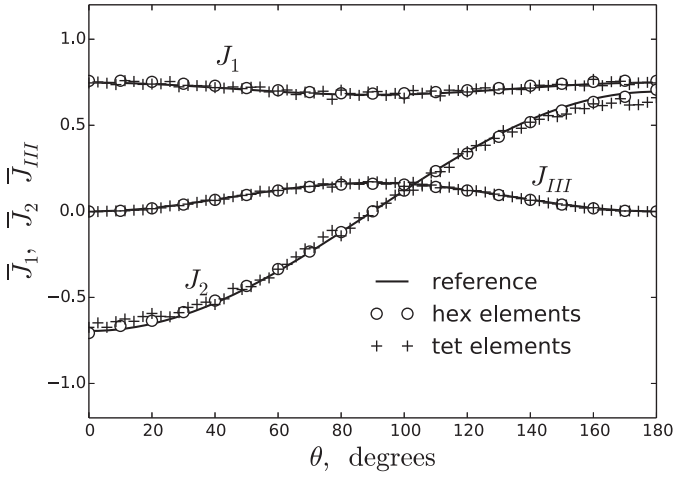

Fig. 19. *J*-integral components at the front of an inclined circular crack under tension.

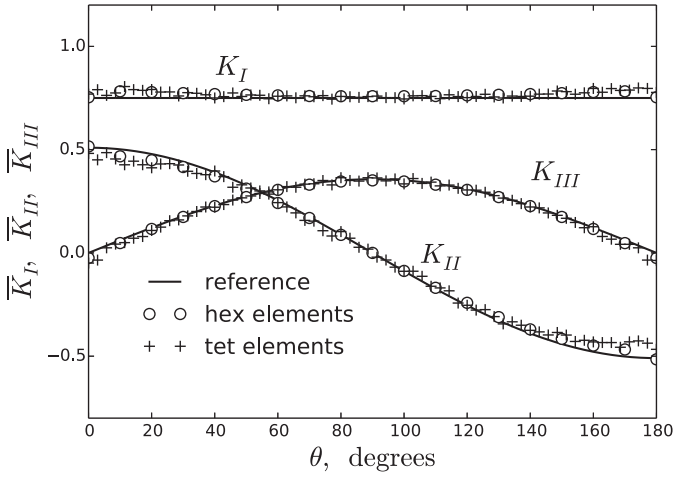

Fig. 20. Stress intensity factors at the front of an inclined circular crack under tension.

Acknowledgement

The research for this article was performed in FIDESYS LLC and financially supported by the Russian Ministry of Education and Science (project No. 14.579.21.0007, unique project identifier RFMEFI57914X0007). The authors are grateful to Professor E.M. Morozov, Moscow Engineering Physics Institute and Professor V.A. Levin, Lomonosov Moscow State University for valuable discussions.

References

[1] Cherepanov GP. The propagation of cracks in a continuous medium. J Appl Math Mech 1967;31:503–12.
[2] Rice JR. A path independent integral and the approximate analysis of strain concentration by notches and cracks. J Appl Mech ASME 1968;35:379–86.
[3] Levin VA, Zingerman KM, Vershinin AV, et al. Numerical analysis of the stress concentration near holes originating in previously loaded viscoelastic bodies at finite strains. Int J Solids Struct 2013;50:3119–35.
[4] Levin VA, Vershinin AV. Non-stationary plane problem of the successive origination of stress concentrators in a loaded body. finite deformations and their superposition. Commun Numer Methods Eng 2008;24:2240–51.
[5] Delorenzi HG. Energy release rate calculations by the finite element methods. Eng Fract Mech 1985;21:129–43.
[6] Li FZ, Shih CF, Needleman A. A comparison of methods for calculating energy release rates. Eng Fract Mech 1985;21:405–21.
[7] Nikishkov GP, Atluri SN. An equivalent domain integral method for computing crack-tip integral parameters in non-elastic, thermo-mechanical fracture. Eng Fract Mech 1987;26:851–67.
[8] Nikishkov GP, Atluri SN. Calculation of fracture mechanics parameters for an arbitrary three-dimensional crack by the equivalent domain integral method. Int J Numer Meth Eng 1987;24:1801–21.
[9] Nikishkov GP. Accuracy of quarter-point element in modeling crack-tip fields. Comput Model Eng Sci 2013;93:335–61.
[10] ANSYS®meshing user guide, release 14.5. ANSYS, inc. 2012.
[11] Rajaram H, Socrate S, Parks DM. Application of domain integral methods using tetrahedral elements to the determination of stress intensity factors. Eng Fract Mech 2000;66:455–82.
[12] Okada H, Ohata S. Three-dimensional J-integral evaluation for cracks with arbitrary curvatures and kinks based on domain integral method for quadratic tetrahedral finite element. Eng Fract Mech 2013;109:58–77.
[13] Chervenka J, Saouma VE. Numerical evaluation of 3-D SIF for arbitrary finite element meshes. Eng Fract Mech 1997;57:541–63.
[14] Nagai M, Ikeda T, Miyazaki N. Stress intensity factor analyses of three-dimensional interface cracks using tetrahedral finite elements. Comput Mech 2013;51:603–15.
[15] Nakamura T, Parks DM. Antisymmetrical 3D stress field near the crack front of a thin elastic plate. Int J Solids Struct 1989;25:1411–26.

[16] Gosz M, Moran B. An interaction energy integral method for computation of mixed-mode stress intensity factors along non-planar crack fronts in three dimensions. Eng Fract Mech 2002;69:299–319.
[17] Nikishkov GP. Estimate of conservativity of elastic approach to elastic-plastic crack problems using two-parameter J-A fracture criterion. Eng Fract Mech 2015;138:92–9.
[18] Eischen JW. An improved method for computing the J_2 integral. Eng Fract Mech 1987;26:691–700.
[19] Walters MC, Paulino GH, Dodds RH Jr. Interaction integral procedures for 3-D curved cracks including surface tractions. Eng Fract Mech 2005;72:1635–63.
[20] Liu GR. Mesh free methods. Moving beyond the finite element method. CRC, Boca Raton; 2003.
[21] Dolbow J, Belytschko T. An introduction to programming the meshless element free galerkin method. Arch Comput Methods Eng 1998;5:207–41.
[22] FIDESYS. Strength analysis system. http://www.cae-fidesys.com/en.
[23] Morozov EM, Levin VA, Vershinin AV. Structural analysis: FIDESYS in engineer's hands. URSS, Moscow 2015:401pp. (in Russian)
[24] Levin VA. Theory of repeated superposition of large deformations: elastic and viscoelastic bodies. Int J Solids Struct 1998;35:2585–600.
[25] Levin VA, Zingerman KM. Interaction and microfracturing pattern for successive origination (introduction) of pores in elastic bodies: finite deformation. ASME J Appl Mech 1998;65:431–5.
[26] Fett T. Stress intensity factors and weight functions for special crack problems, FZKA 6025. Forschungszentrum Karlsruhe; 1998.
[27] Sneddon IN, Lowengrub M. Crack problems in the classical theory of elasticity, The SIAM series in applied math. Wiley, NY; 1969.
[28] Newman JC, Raju IS. Stress intensity factor equation for cracks in three-dimensional finite bodies subjected to tension and bending loads. National Aeronautics and Space Administration, Langley Research Centre, Hampton, VA; 1984. Report nasa-tm-85793.
[29] Kassir MK, Sih GC. Three-dimensional stress distribution around an elliptical crack under arbitrary loading. ASME J Appl Mech 1966;33:601–11.